Investigation on the Arrangement of Lithium Ions in $Li_xLa_{1/3}NbO_3$ with Perovskite Structure

Masanobu Nakayama,[†] Masataka Wakihara,[†,*] Yo Kobayashi,[‡] and Hajime Miyashiro[‡]

Department of Applied Chemistry, Tokyo Institute of Technology, Ookayama, Meguro-ku, Tokyo 152-8552, Japan, and Materials Science Research Laboratory, Central Research Institute of Electric Power Industry, 2-11-1, Iwado Kita, Komae-shi, Tokyo 201-8511, Japan

Received: April 25, 2005; In Final Form: June 2, 2005

The relationship between the Li arrangement and the electrochemical behavior has been examined as a function of composition x in electrochemically lithiated A-site deficient perovskite, $Li_xLa_{1/3}NbO_3$. The cell potential diagram and powder X-ray diffraction (XRD) study indicated that the Li ions are inserted into the vacant Perovskite A-site with an electrochemical reaction. In addition, the derivatives of the cell potential diagram showed three cathodic peaks, indicating a stepwise Li insertion mechanism takes place. Such a stepwise behavior would be ascribed to the changes in arrangement of inserted Li ions in the Perovskite lattice, since the XRD patterns of pristine $La_{1/3}NbO_3$ showed that the La arrangement in $La_{1/3}NbO_3$ was ordered along the c-axis, causing two kinds of A-site vacancies. To reveal the changes in the arrangement of Li ions, the entropy measurement of the reaction was performed by both the electrochemical and the calorimetric techniques. Moreover, the formation energy of the Perovskite structure with various Li arrangements was compared by using an ab initio calculation. The results of experiment and computation suggested that the electrochemical reaction proceeded via two kinds of superstructures of $Li_{1/6}La_{1/3}NbO_3$ and $Li_{1/2}La_{1/3}NbO_3$ due to the ordered arrangement of Li ions.

Introduction

The electrochemical lithium insertion technique is a method with particular significance to high-energy dense electrode materials to be used for lithium ion batteries.[1,2] Materials having lithium insertion sites are attractive not only to be used for practical purposes but also to be used as a model material in the fundamental study of solid-state electrochemical reactions. This originates from the two reasons described as follows: (1) the host crystal structure remained almost unchanged before and after the electrochemical reaction[2] and (2) the molar amount of reacted species, the free energy of the reaction, and kinetic parameters such as diffusion coefficient can easily be estimated by monitoring the cell voltage and electronic current.

A-site deficient perovskite oxide, $La_{1/3}NbO_3$, is considered to be one of the candidates of a model compound, because there are a large number of vacancies to insert Li ions, almost no side reaction is observed in this reaction, etc.[3−8] In this respect, we have recently investigated the Li insertion mechanism in view of long-range electrostatic interaction,[4] changes in electronic structure,[5,6] local structural modification,[7] and electrode−electrolyte interfacial reaction.[8] From these studies, useful and general knowledge regarding the lithium insertion was extracted. However, there is a disadvantage in this kind of fundamental investigation that the detection and the estimation of the location of inserted lithium ions are usually difficult due to experimental limitations, such as the low X-ray scattering ability of Li.

One of the solutions for this issue is the measurement of the entropy of reaction. The entropy of reaction reflects mainly the configurational entropy of the Li ion arrangement, or the degree of order or disorder of the lithium arrangement in the lattice, under the assumption that the host lattice keeps its structural framework during the reaction. Therefore, the entropy measurement would provide the lithium arrangement (for example, see refs 9−12). In addition, it is relatively easy to obtain thermodynamic functions in the electrochemical system, since the derivative of the open-circuit potential (OCP), E_{eq}, with respect to the temperature, dE_{eq}/dT, is proportional to the entropy of reaction as expressed by following equation,

$$dE_{eq}/dT = \Delta S_{obs}/nF \quad (1)$$

where n is the number of electrons denoted in the electrochemical reaction (in the case of Li insertion, $n = 1$), F is Faraday's constant, and ΔS_{obs} is the observed entropy of reaction.

In present paper, to clarify and demonstrate the detailed lithium distribution in $Li_xLa_{1/3}NbO_3$ as a function of composition x, the entropy of reaction was measured by a dual method, the electrochemical and the calorimetric techniques. In addition, the ab initio band calculation based on the density functional theory was carried out to reveal the arrangement of Li ions in view of the calculated formation energy.

Structure Description

So far, the host structure itself has been investigated mainly by using diffraction technique. The crystal structure of the parent, $La_{1/3}NbO_3$, was first described by Iyer et al.[13] and later by Turnov et al.[14] As shown in Figure 1, La ions and vacancies at A-sites are ordered within alternate (001) planes doubling the c parameter of the cubic perovskite type cell and leading to a slightly distorted orthorhombic lattice with parameters $a \sim a_p$, $b \sim a_p$, $c \sim 2a_p$ (subscript "p" refers to the primitive

* Address correspondence to this author. Phone: +81-3-5734-2145. Fax: +81-3-5734-2146.
[†] Tokyo Institute of Technology.
[‡] Central Research Institute of Electric Power Industry.

10.1021/jp052142r CCC: $30.25
Published on Web 07/08/2005

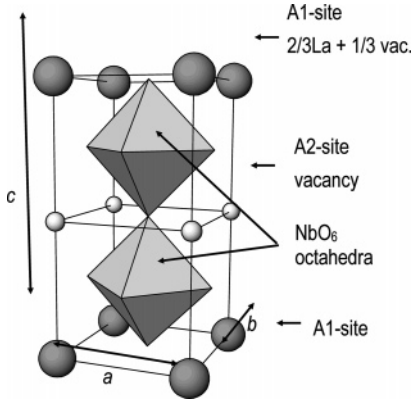

Figure 1. Crystal structure of $La_{1/3}NbO_3$.

perovskite unit cell with $Pm\bar{3}m$ symmetry). Therefore, two kinds of A-site exist in this structure, and hereinafter the A-site with La-rich and La-poor layers are denoted as the A1-site and the A2-site, respectively (see Figure 1).

On the other hand, there is limited information on the crystal structure of electrochemically Li inserted material. Nadiri et al.[3] confirmed that the host structure of $Li_xLa_{1/3}NbO_3$ is maintained during the insertion reaction, and reported the lattice parameters with composition x using X-ray diffraction (XRD) measurement, and Dilanian et al.[15] investigated the crystal structure of chemically lithiated perovskite oxides, $Li_xLa_{1/3}NbO_3$ ($x = 0$, 0.075), using the neutron diffraction (ND) technique. We have recently investigated the electrochemical behavior with Li insertion into the solid solution $Li_yLa_{(1-y)/3}NbO_3$, and concluded that the cell potential behavior with Li insertion strongly depends on the arrangement of La.[4] These three reports[3,4,15] agree with their conclusion that the inserted lithium ions reside at the vacant A-site of $La_{1/3}NbO_3$. In addition, our report proposed that stepwise reaction took place in $Li_xLa_{1/3}NbO_3$ (La ordered structure) where A1-site vacancies were initially filled with lithium ions, and then lithium ions inserted into A2-site vacancies. However, our proposal is only based on the indirect interpretation of electrochemical behavior.

Model

Three routes for reaction procedure can be proposed for the electrochemical lithium insertion as follows: (route 1) Li ions insert into A-sites randomly regardless of the differece in A1 and/or A2 vacancies, (route 2) Li ions insert initially into A1-site vacancies and then into A2-site, and vice versa (route 3). Theoretically, the configurational entropy, S_{conf}, arising from the arrangements of the vacancies and the lithium ions can be easily calculated by following equation,

$$S_{conf}/k = \frac{N \ln N}{n_{Li} \ln n_{Li} \cdot n_{vac} \ln n_{vac}} \qquad (2)$$

where k is the Boltzmann constant, and n_{Li} and n_{vac} are the numbers of lithium ions and vacancies, respectively. N is the total site number and equal to ($n_{Li} + n_{vac}$) in this case. (This equation assumed the condition that A-site cations (Li and La) in the same crystallographic site do not interact each other.) Moreover, since the experimental results of ΔS_{obs} correspond to the derivative of S_{conf} with respect to the composition x, the derivative of configurational entropy for each of the three routes would be expressed as shown in Figure 2. Therefore, the route of the electrochemical Li insertion reaction would be determined by the comparison of experimental results with the theoritical results in Figure 2.

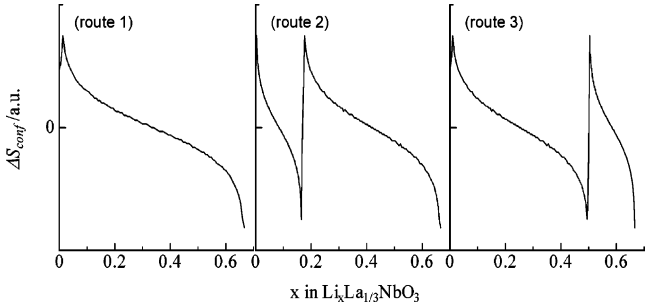

Figure 2. The theoretical configurational entropy of reaction as a function of lithium content in $La_{1/3}NbO_3$. The fFollowing three cases are assumed in this calculation: (1) Li ion inserts into all A-sites randomly without a stepwise reaction, (2) Li ion inserts initially into A1-site vacancies and then into the A2-site, and (3) Li insertion takes place in the opposite manner of case (2).

Experimental Section

The parent material, $La_{1/3}NbO_3$, was prepared by conventional solid-state reaction along with the method described in ref 16. The mixture of stoichiometric amounts of La_2O_3 (3 N) and Nb_2O_5 (3 N) was heated at 800 °C for 2 h and then at 1300 °C for 24 h in air with several intermittent grindings. The phase identification and the evaluation of lattice parameters were carried out by powder XRD technique, using Cu Kα radiation (RINT-2500V, Rigaku Co. Ltd). Rietveld analysis was performed for the prepared sample at room temperature with use of the RIETAN-2000 profile refinement program.[17]

The slow speed galvanostatic electrochemical Li insertion was carried out with use of a three-electrode cell with a current density of 20 μA/cm^2. Li foil (Aldrich) was used as the counter and the reference electrodes and a 1 M solution of $LiClO_4$ in anhydrous ethylene carbonate (EC) and diethylene carbonate (DEC) was used as the electrolyte (Tomiyama Pure Chemical Company, Limited). The working electrode was the mixture of 90 wt % of perovskite powder, 7 wt % of acetylene black as a current collector, and 3 wt % of poly(tetrafluoroethylene) (PTFE) binder. Li foils and the working electrode mixture were pressed onto Ni-mesh. Crystalline phase identification for $Li_xLa_{1/3}NbO_3$ was carried out by powder XRD, using Cu Kβ radiation. In this measurement, the Ni powder was used as an internal standard material, and the sample was covered with polyethylene film in an Ar-filled glovebox to prevent reactions with moisture in the atmosphere.

The entropy of the reaction was measured by a dual method: electrochemical and calorimetrical techniques. The electrochemical one was performed along with the method reported by Thomas et al.[9] Coin type cells were used to obtain good heat conduction. For the working electrode, perovskite powder was mixed with acetylene black as a current collector and polyvinyliden binder at a weight ratio of 8:1:1, and the slurry was made with *N*-methylpyrrolidone (NMP) solvent. The slurry was coated onto a copper sheet, dried under vacuum at 60 °C, and cut into a disk. This disk and a foil of lithium metal were used as the working and counter electrodes, respectively. The 1 M solution of $LiClO_4$ in anhydrous propylene carbonate (PC) was used as the electrolyte (Tomiyama Pure Chemical Company, Limited). Before the entropy measurement, the cells were cycled with a cutoff voltage 1.0 to 2.2 V to complete an irreversible side reaction, such as organic film formation on the surface of the electrode materials and so on. Then, the cells were discharged at a constant current of 0.1 mA/cm^2 to the various compositions x in $Li_xLa_{1/3}NbO_3$ at 298 K in a thermostat. After the discharging, the cells were relaxed 12 h, and their

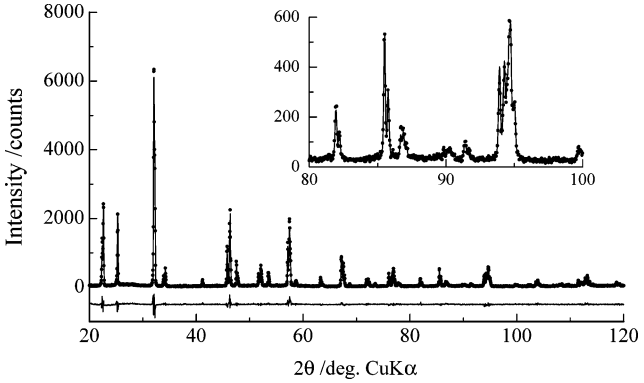

Figure 3. Observed (solid circle) and calculated (solid line) XRD patterns for Rietveld analysis. The differential pattern is also shown at the bottom of this figure.

OCP were checked. The composition x was again evaluated with use of the OCP data reported previously[4] to avoid the compositional error arising from the quite small amount of active material used in a coin type cell. The temperature was varied following three steps: (1) increase the temperature from 298 to 303 K at a rate of 25 K/h, (2) decrease from 303 to 293 K at 25 K/h, and (3) return to 298 K at 25 K/h, then relaxed for 6 h. (These three steps were also repeated for some of the samples at a rate of 5 K/h to check the effect of thermal conduction for the cell, and good reproducibility was obtained with respect to the value of the entropy change.) The OCP and temperature were monitored every 10 s. Note that, although the cells were relaxed 12 h after the end of the discharge process, the observed potential profile shows a gradual increase (ca. +0.001 V/h). To correct for the continual increase of the cell potential, the potential profile of 298 K before and after temperature cycling was extrapolated by parabolic functions. The obtained potential profile during temperature cycling was subtracted from the approximated parabolic functions, and then the differential potential curve was obtained. This differential potential was plotted as a function of temperature, and then fitted by the linear function.

The entropy measurement by the calorimetric technique was carried out as follows. The heat flow during lithium insertion was measured with a Calvet-type conduction microcalorimeter (MMC-5111-U Tokyo Riko, Tokyo). The detailed description of the calorimeter and related apparatus have already been presented in refs 18 and 19. The two-electrode-type coin cell mentioned above was used for the calorimetric measurement. The heat flow was measured during the electrochemical lithium insertion with a current density of 0.1 mA/cm^2, at 298 K. The heat flow was converted to the entropy of the reaction, dS_{obs}, using the following relationship

$$\Delta S_{obs} = \frac{Q \cdot F}{I \cdot T} \qquad (3)$$

where Q, F, I, and T indicate the heat flow, Faraday constant, current, and temperature, respectively.

Results and Discussion

Solid circles in Figure 3 show the observed XRD patterns of prepared perovskite structure, $La_{1/3}NbO_3$, and only the perovskite phase with orthorhombic symmetry was observed. Structure refinement was carried out with Rietveld analysis. The space group, *Pmmm* for $La_{1/3}NbO_3$, was used to take into account the orthorhombic symmetry and to refer to the previous reports.[7] In this model, La ions are distributed in two sites, La1 and La2,

TABLE 1: Structural Parameters of $La_{1/3}NbO_3$ Obtained by the Rietveld Analysis for the XRD Data[a]

label/ atom	site	site occupancy g	x	y	z	B/Å^2
La1/La	1a (A1)	0.661(2)	0(−)	0(−)	0(−)	0.09(1)
La2/La	1b (A2)	0.006(−)	0(−)	0(−)	0.5(−)	0.09(−)
Nb/Nb	2t	1.0(−)	0.5(−)	0.5(−)	0.2605(2)	0.47(4)
O1/O	2r	1.0(−)	0(−)	0.5(−)	0.226(3)	0.63(14)
O2/O	2s	1.0(−)	0.5(−)	0(−)	0.239(3)	0.63(−)
O3/O	1f	1.0(−)	0.5(−)	0.5(−)	0(−)	0.63(−)
O4/O	1h	1.0(−)	0.5(−)	0.5(−)	0.5(−)	0.63(−)

[a] Each refinement quality parameter is defined as follows: $R_{wp} = [\sum_i w_i(y_{i,obs} - y_{i,cal})^2/\sum_i w_i y_{i,obs}]^{1/2}$, $R_p = \sum_i |y_i - f_i(x)|/\sum_i y_i$. $La_{1/3}NbO_3$ in *Pmmm* (unit cell; $La_{2/3}Nb_2O_6$, see Figure 1. Lattice parameters: a = 3.91093(89) Å, b = 3.92022(89) Å, c = 7.91388(181) Å, $\alpha = \beta = \gamma = 90°$. Cell volume: V = 121.3333(479) Å^3. Reliability parameters: R_{wp} = 14.40%, R_P = 10.37%, $S = (R_{wp}/R_e)$ = 1.4810.

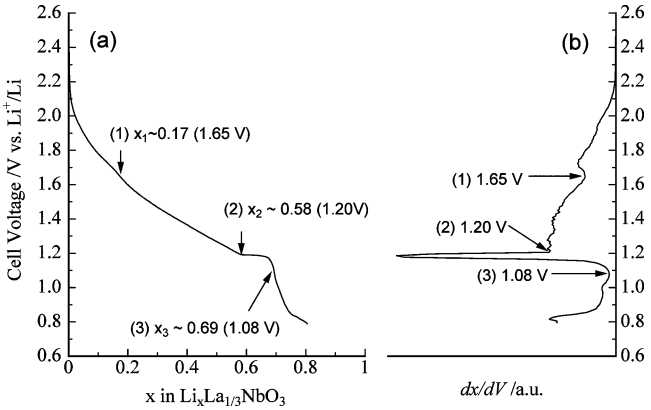

Figure 4. (a) Variation of the cell potential versus molar amount of inserted lithium ions (20 μA/cm^2) and (b) derivative curves of the amount of inserted lithium ions with cell potential.

which correspond to the A1-site and the A2-site in Figure 1, respectively. The site occupancy parameters g of La ions in both of the A-sites were constrained along with the requirement of chemical formula. (That is to say, the refinement of g parameters in $La_{2/3}Nb_2O_6$ was carried out under the constraints of g(La1) + g(La2) = $^2/_3$.) Debye−Waller coefficients B(La) and B(O) for two La sites and four O sites were fixed to be the same values, respectively. The results are listed in Table 1, and the simulated patterns are superimposed in Figure 3. The validity of the Rietveld analysis was supported by the relatively small refinement quality parameters, R_{wp} and R_p, listed in Table 1 and by good accordance between the calculated and experimental XRD patterns (Figure 3). As seen in Table 1, it was confirmed that almost all La ions are distributed in the A1-site, while no cations existed in the A2-site in the perovskite structure in $La_{1/3}NbO_3$.

The slow speed galvanostatic discharge and its derivative curves for the $Li_xLa_{1/3}NbO_3$ electrochemical system were presented in Figure 4 , parts a and b, respectively. The obtained discharge curves were almost the same as observed in OCP measurements reported previously[4] at the range of $0 < x < 0.7$. The derivative curve in Figure 4b showed three cathodic peaks, indicating the three-step insertion reactions in this electrochemical reaction system. The voltage where each reaction terminated was determined as (1) 1.65, (2) 1.20, and (3) 1.02 V, respectively, as shown by the arrow in Figure 4b. The corresponding compositions x in $Li_xLa_{1/3}NbO_3$ were also obtained as follows: (1) x = 0.17, (2) x = 0.58, and (3) x = 0.69. Since composition (1), x = 0.17, corresponded to the molar amount of A1-site vacancies, the A1-site was initially occupied by the inserted lithium ions as proposed in the previous paper.[4]

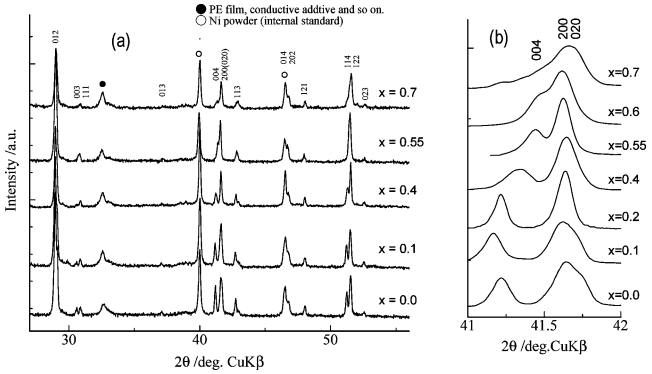

Figure 5. Powder XRD patterns of the perovskite compounds, $Li_xLa_{1/3}NbO_3$.

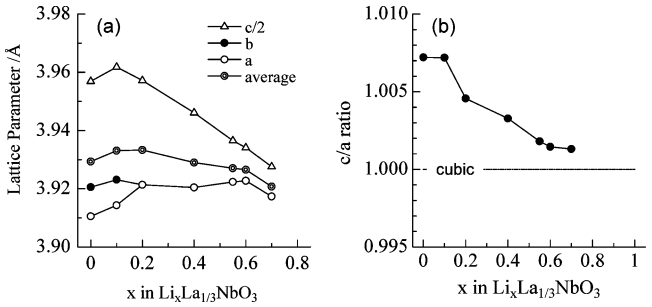

Figure 6. (a) Refined lattice parameters versus x in $Li_xLa_{1/3}NbO_3$ and (b) variation of c/a ratio during the lithium insertion.

The flat plateau started from composition (2), $x = 0.58$, and would arise from two-phase coexistence. Finally, the lithium insertion reaction is terminated at composition (3), $x = 0.69$, where the large potential drop was observed, indicating that all the vacancies were filled with electrochemically inserted Li ions. Since composition (3) agrees with the total molar amount of A-site vacancies in $La_{1/3}NbO_3$, Li ions inserted into the A-site vacancies as mentioned above.

The structural change with lithium insertion was evaluated by ex situ XRD, and the results were shown in Figure 5. As shown in Figure 5a, the peak feature of the patterns was roughly unchanged with Li insertion, so that the host structure of $La_{1/3}NbO_3$ keeps its framework upon Li insertion. In detail, the peaks of 200 and 020 were incorporated initially, and then those of 200 and 004 tend to gather with Li insertion (see Figure 5b; a similar behavior is also observed in the peaks of 114 and 122). The refined lattice parameters are shown in Figure 6a, and their variation with composition x agrees with the results reported by Nadiri et al.[3] The c/a ratio in Figure 6b, which represents the tetragonal distortion defined as half of the c-axis was divided by averaged lattice parameters of a and b, shows a decrease toward 1.0 (cubic) with lithiation. This distortion along the c-axis would be due to the La ordering or to the fact that the positive charge of La^{3+} distributed in the A1-site solely, and no charged particles exist in the A2-site in the perovskite structure. Therefore, decreasing the c/a ratio would be ascribed to decreasing the anisotropic distribution of the positive charge between the A1- and A2-site, since the lithium ion inserts into the A2-site. In this point of view, if the lithium ion initially inserts into the A1-site up to the composition $x = 1/6$ as mentioned above, the c/a ratio would increase from $x = 0$ to 1/6 and then decrease with lithium insertion. Figure 6b seems to support this assumption, because the c/a ratio does not decrease at the range of $x < 1/6$. However, it is difficult to conclude due to insufficient data and quality. Adopting an advanced diffraction investigation, such as in situ XRD technique, twould be needed to eliminate the geometrical error of optical setting (note that the ex situ technique cannot keep the same geometrical condition for each measurement).

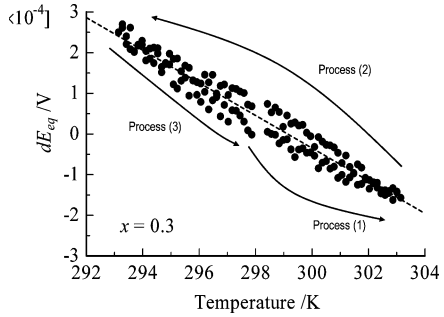

Figure 7. Example of the variation of differential potential with regard to the temperature. The slope of this curve (hatched line), dE_{eq}/dT, is proportional to the entropy of reaction. Processes (1) to (3) indicate the temperature cycling operations over time (described in the Experimental Section).

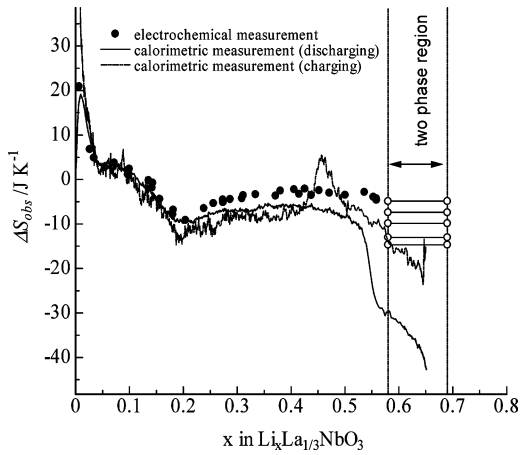

Figure 8. The observed entropy of reaction as a function of lithium content in $La_{1/3}NbO_3$. Solid dots show the entropy obtained by the electrochemical measurement, while lines indicate those obtained by the calorimetric measurement (solid line: discharging; and hatched line: charging).

Figure 7 shows an example of the variation of differential potential versus temperature. As shown in the figure, the potential change against the temperature was approximated to a linear function, and its gradient, dE_{eq}/dT, was converted to the entropy of reaction, ΔS_{obs}, using eq 1. (Note that the obtained ΔS_{obs} includes the contribution of the redox reaction at the counter electrode as well as that in the working electrode.) The obtained ΔS_{obs} was plotted as a function of composition x in Figure 8. The ΔS_{obs} initially decreases with lithiation up to $x \sim 0.2$, and then convex-shaped curves were observed in the range of $\sim 0.2 < x < 0.58$. In the range of $0.58 < x < 0.69$ where the two-phase coexistence type reaction proceeds, the ΔS_{obs} was plotted at both compositions $x = 0.58$ and 0.69 by open circles connected with a line to each other, because it is difficult to evaluate the accurate composition of x by OCP (see the Experimental Section) due to the constant value with respect to the composition x. The entropy of the reaction obtained by the calorimetric method is also presented in Figure 8. As seen in the figure, good accordance was obtained between the electrochemical and the calorimetric methods up to the composition $x < \sim 0.5$. Therefore it was confirmed that both of the methods are reliable enough to measure the entropy of reaction in $Li_xLa_{1/3}NbO_3$ systems, especially in the compositional range of $0 < x < 0.5$. On the other hand, the observed entropy of reaction, ΔS_{obs}, showed different behavior between calorimetric

TABLE 2: Crystal Structure of $Li_xLa_{1/3}NbO_3$[a] ($x = 0$, 1/6, 1/2, 2/3) for ab Initio Calculation

label/atom	no. of sites	fractional coordinates		
		x	*y*	*z*
La1/La	1	0	0.5	0.5
Nb1/Nb	4	0.5	0.25	1/3
Nb2/Nb	2	0.5	0.25	0
O1/O	4	0.5	0.25	1/6
O2/O	4	0	0.25	2/3
O3/O	2	0.5	0.25	0.5
O4/O	2	0	0.25	0
O5/O	2	0.5	0	1/3
O6/O	1	0.5	0	0
O7/O	2	0.5	0.5	1/3
O8/O	1	0.5	0.5	0
Li1/Li[b]	2	0	0.5	1/6
Li2/Li[c]	2	0	0	1/6
Li3/Li[c]	1	0	0	0.5

[a] Space group: *Pmmm* (no. 47). Lattice parameters: $a = 3.930$ Å, $b = 7.860$ Å, $c = 11.790$ Å, $\alpha = \beta = \gamma = 90°$. [b] A1-site (considered for the composition $x = 1/6$, 2/3). [c] A2-site (considered for the composition $x = 1/2$, 2/3.

and electrochemical measurement in the composition of $x > \sim 0.5$, including a two-phase coexisting region. Moreover, ΔS_{obs} obtained by the calorimetric method disagreed in this composition between charging and discharging. Therefore, one of the considerable reasons for the discrepancy is that the observed entropy change by the calorimetric method does not reflect the equilibrium state of $Li_xLa_{1/3}NbO_3$ in this range due to the following experimental difference: the measurement of the electrochemical method was carried out after the relaxation of the discharge reaction, while that of the calorimetric method was performed under the dynamic discharge/charge reaction.

Hereafter, we discuss the details of the change in the entropy of reaction. The values of the entropy of reaction are positive when the lattice is mostly empty ($0 < x < 0.1$), show a transition to negative from the composition $x \sim 0.1$, and then show anomalous change (slight increase) from $x \sim 0.2$. In this region ($0 < x < 0.2$), the qualitative behavior of the entropy of the reaction is similar to that of the model (route 2) shown in Figure 2. Therefore, it was confirmed that the lithium ion selectively inserted into the A1-site in this region as suggested in previous papers.[4,15] On the other hand, the values of the entropy of reaction are slightly negative (almost zero) in the intermediate composition of $\sim 0.2 < x < \sim 0.6$. Such a behavior indicates the discrepancy from route 2, since the entropy of reaction is expected to become positive again at the composition $x \sim 0.2$, where the Li ions begin to insert into A2-site vacancies (see Figure 2, route 2). Therefore the observed changes in the entropy of reaction cannot be explained simply by the model of route 2.

To clarify the unexpected change of the entropy of reaction, ab initio band calculation based on the density functional theory was performed with use of the program package Wien2k.[19] The detailed procedure in this calculation is described elsewhere.[20] The total energy of the four different compositions, $La_{1/3}NbO_3$, $Li_{1/6}La_{1/3}NbO_3$ (all A1-sites are filled with Li ions), $Li_{1/2}La_{1/3}NbO_3$ (all A2-sites are filled with Li ions), and $Li_{2/3}La_{1/3}NbO_3$ (all A-site vacancies are filled with Li ions), was calculated. The structural information for the calculation was tabulated in Table 2. Since the change in the lattice parameter upon electrochemical lithiation is quite small as shown in Figure 5 (the cell volume decreased only ~0.3% versus the $La_{1/3}NbO_3$ unit cell after lithium insertion), the constant volume assumption was adopted

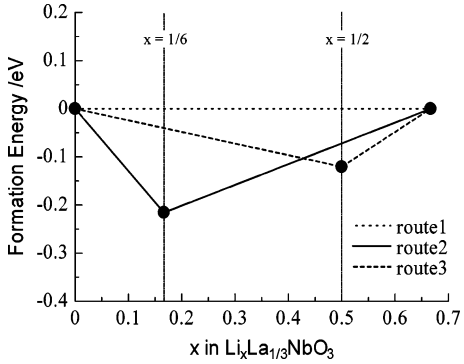

Figure 9. The variation of the calculated formation energy versus composition x in $Li_xLa_{1/3}NbO_3$.

for the calculation. To evaluate the relative structural stability, the formation energies, $\Delta_f E$, are defined as

$$\Delta_f E = E(Li_xLa_{1/3}NbO_3) - xE(La_{1/3}NbO_3) - (1 - x)E(Li_{2/3}La_{1/3}NbO_3) \quad (4)$$

where E(A) is the total energy of A per $Li_xLa_{1/3}NbO_3$ formula unit (the definition of the formation energy is described elsewhere, see ref 21). The results of ab initio calculations are plotted in Figure 9. Three routes were assumed regarding the lithium insertion as mentioned in the Model section: (route 1) Li ions insert randomly into A-site vacancies regardless of the distinction of A1- and A2-vacancy, (route 2) Li ions insert into the A1-site vacancies initially, and then occupy A2-site vacancies, and (route 3) Li ions insert in the opposite manner of route 2. Due to the limitation of computational resources, the formation energy of intermediary composition was extrapolated linearly for each route (see Figure 9). (This assumption indicates that the Li ions insert in the manner of a two phase reaction between two compositional materials. However, since the experimental potential profile clearly showed the solid-state-type reaction at the range of $x < 0.58$, the formation energy of the intermediate composition should be lower than the line presented in Figure 9.) As seen in Figure 9, the expected formation energy of route 1 products is larger than that of route 2 and route 3 products in the whole compositional range. Therefore the superstructures of $Li_{1/6}La_{1/3}NbO_3$ and/or $Li_{1/2}La_{1/3}NbO_3$ would be stable in this reaction, or the lithium ions do not randomly insert into both A1- and A2-sites. In detail, at the composition $x = 1/6$, the most stable phase is the route 2 structure (A1-sites are filled with Li, while A2-sites consist of vacancies). Therefore, ab initio calculation supports the experimental electrochemical behavior at the range of $0 \le x \le 1/6$, and it was indicated that Li ions selectively insert into the A1-site. On the other hand, at the composition $x = 1/2$, route 3 product seems to be the stable one rather than that of route 2. Hence, the calculated results indicate that Li ions occupied the A1-site initially up to composition $x = 1/6$, then the Li ions migrate into the A2-site with further Li insertion, and finally whole lithium ions reside in the A2-site at the composition $x = 1/2$. Thus, it was suggested that the discrepancy of the entropy change between observation (Figure 8) and simulation (Figure 2b) in the range of $\sim 0.2 \le x \le \sim 0.4$ might be ascribed to the effect of Li redistribution between the A1-site and the A2-site. Moreover, the two-phase reaction at the range of $x > 0.58$ would be related to the superstructure of $Li_{1/2}La_{1/3}NbO_3$ where all Li ions reside in the A2-site.

To confirm the suggestion of ab initio results, the configurational entropy was recalculated with use of eq 2 along with

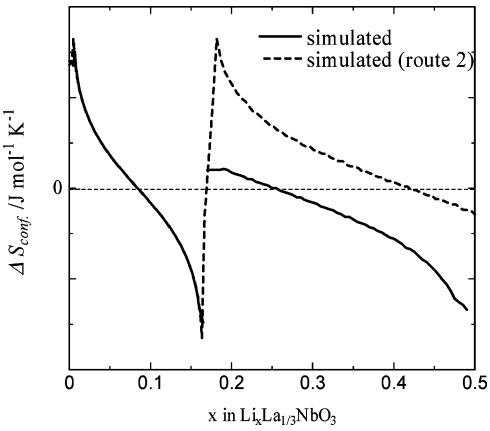

Figure 10. Calculated (configurational) entropy of reaction as a function of x in $Li_xLa_{1/3}NbO_3$. The solid line indicates the changes in the entropy of reaction indicatied by ab initio computation, while the hatched line indicates the one based on the reaction (route 2) shown in Figure 2.

the extreme assumption as the following three-step reaction in the range of $0 \leq x \leq 0.5$: (1) the Li ions initially insert into the A1-site up to $x = 1/6$, (2) all Li ions migrate to the A2-site, once additional lithium insert into the $Li_{1/6}La_{1/3}NbO_3$ structure, and then (3) Li ions insert into the A2-site. The calculated configurational entropy (derivative form) is shown in Figure 10. The changes in configurational entropy at $x = 1/6$ are a little positive, showing similar behavior to experimental data rather than calculated data of route 2. Maybe the deviation between modeled and observed entropy of reaction remaining still could be ascribed to the fact that the calculated entropy assumed the extreme condition, all Li ions migrate from the A1-site to the A2-site at the composition $x = 1/6$, and eq 2 also assumed that the inserted Li ions do not interact with each other. In actual system, it was expected the occupancy of Li ions at A1 and A2-site would be gradually change around $x = 1/6$. Summing up the above discussion, it was suggested that lithium ion insertion into the Perovskite structure proceeded via two superstructures of $Li_{1/6}La_{1/3}NbO_3$ and $Li_{1/2}La_{1/3}NbO_3$ (A1- and A2-sites were filled by Li, respectively).

Finally we dicuss the descrepancy observed in the calorimetric method between charging and discharging. Especially in the charging process, the sign of the entropy of reaction varies around the two-phase coexisiting region ($x > \sim 0.5$). Such behavior could be ascribed to the selective Li extraction from the A1-site in this compositional range in view of the assumption above (Figures 9 and 10). In addition, the amount of Li extraction agreed with that of the Li/vacancy site in the A1-site. Thus, the observed behavior would support the assumption above, if the solid−solution-like reaction proceeded in the dynamic charging process at the compositional range of $x > 0.5$.

In conclusion, the distribution of electrochemically inserted lithium in the lattice was investigated by the entropy measurement of the reaction. The experimental results clearly showed a stepwise reaction where lithium inserted initially into the A1-site and then into the A2-site at the composition $x \sim 0.17$ and agree with simulated entropy change. In addition, good accordance was observed in the entropy measurement between electrochemical and calorimetric techniques, indicating the method presented in this paper is accurate and powerful enough to discuss the distribution of inserted lithium ions.

Acknowledgment. This work was supported by Grant-in-Aid for Scientific Research on Priority Areas (B) (No.740) "Fundamental Studies for Fabrication of All Solid State Ionic Devices" from the Ministry of Education, Culture, Sports, Science and Technology. One of the authors, M.N., would like to thank the Japan Society for the Promotion of Science for financial support of this work.

References and Notes

(1) Scrosati, B. *Nature* **1995**, *573*, 557.
(2) Wakihara, M.; Li, G.; Ikuta, H. *Lithium Ion Batteries*; Kodansha: Tokyo, Japan, 1998; Chapter 2.
(3) Nadiri, A.; Flem, G. L.; Delmas, C. *J. Solid State Chem.* **1988**, *73*, 338.
(4) Nakayama, M.; Imaki, K.; Ikuta, H.; Uchimoto, Y.; Wakihara, M. *J. Phys. Chem. B* **2002**, *106*, 6437.
(5) Nakayama, M.; Imaki, K.; Ra, W.-K.; Ikuta, H.; Uchimoto, Y.; Wakihara, M. *Chem. Mater*. **2003**, *15*, 1728.
(6) Nakayama, M.; Ra, W.-K.; Ikuta, H.; Uchimoto, Y.; Wakihara, M. *Electrochemistry* **2003**, *71*, 1025.
(7) Nakayama, M.; Ikuta, H.; Uchimoto, Y.; Wakihara, M.; Terada, Y.; Miyanaga, T.; Watanabe, I. *J. Phys. Chem. B* **2003**, *107*, 10715.
(8) Nakayama, M.; Ikuta, H.; Uchimoto, Y.; Wakihara, M. *J. Phys. Chem. B* **2003**, *107*, 10603.
(9) Thomas, K. E.; Bogatu, C.; Newman, J. *J. Electrochem. Soc.* **2001**, *148*, A570.
(10) Thomas, K. E.; Newman, J. *J. Power Sources* **2003**, *119*−*121*, 844.
(11) Barbato, S.; Gautier, J. L. *Electrochim. Acta* **2001**, *46*, 2767.
(12) Kim, S.-W.; Pyun, S.-I. *Electrochim. Acta* **2001**, *46*, 987.
(13) Iyer, P. N.; Smith, A. J. *Acta Crystallogr.* **1967**, *23*, 740.
(14) Trunov, V. K.; Averina, I. M.; Evdokimov, A. A.; Frolov, A. M. *Kristallografiya* **1981**, *261*, 189.
(15) Dilanian, R. A.; Yamamoto, A.; Izumi, F.; Kamiyama, T. *Mol. Cryst. Liq. Cryst.* **2000**, *341*, 225.
(16) Kawakami, Y.; Ikuta, H.; Wakihara, M. *J. Solid State Electrochem.* **1998**, *2*, 206.
(17) Izumi, F.; Ikeda, T. *Mater. Sci. Forum* **2000**, *321*−*324*, 198.
(18) Kobayashi, Y.; Kihira, N.; Takei, K.; Miyashiro, H.; Kumai, K.; Terada, N.; Ishikawa, R. *J. Power Sources* **1999**, *81*−*82*, 463. Kobayashi, Y.; Miyahiro, H.; Kumai, K.; Takei, K.; Iwahori, T.; Uchida, I. *J. Electrochem. Soc.* **2002**, *149*, A978.
(19) Blaha, P.; Schwarz, K.; Sorantin, P.; Trickey, S. B. *Comput. Phys. Commun.* **1990**, *59*, 399. Blaha, P.; Schwarz, K.; Madsen, G. K. H.; Kvasnicka, D.; Luitz, J. *WIEN2k*, Vienna University of Technology, An Augmented Plane Wave + Local Orbitals Program for Calculating Crystal Properties revised edition 2001 (for further details see, for example, the documentation at the URL: http://www.wien2k.at).
(20) Nakayama, M.; Imaki, K.; Uchimoto, Y.; Wakihara, M. *Solid State Ionics* **2004**, *172*, 77. Nakayama, M.; Usui, T.; Uchimoto, Y.; Wakihara, M.; Yamamoto, M. *J. Phys. Chem. B* **2005**, *109*, 4135.
(21) Van der Ven, A.; Ceder, G. *Phys. Rev. B* **1999**, *59*, 742.